Journal of Nuclear Medicine, published on February 14, 2020 as doi:10.2967/jnumed.119.240424

2Intraoperative ^{68}Gallium-PSMA Cerenkov Luminescence Imaging for surgical margins in radical prostatectomy – a feasibility study

Cerenkov Luminescence in radical prostatectomy

Darr C[1*], Harke NN[1*], Radtke JP[1], Yirga L[1], Kesch C[1], Grootendorst MR[2], Fendler WP[3], Fragoso Costa P[3], Rischpler C[3], Praus C[3], Haubold J[4], Reis H[5], Hager T[5], Herrmann K[3], Binse I[3†*], Hadaschik BA[1*]

[*] Contributed equally
† died during the preparation of the manuscript

1 - Department of Urology, University Hospital Essen, Essen, Germany[6]
2 - Clinical Research, Lightpoint Medical Ltd., Chesham, United Kingdom
3 - Department of Nuclear Medicine, University Hospital Essen, Essen, Germany[6]
4 - Institute of Diagnostics and Radiology, University Hospital Essen, Essen, Germany[6]
5 - Institute of Pathology, University Duisburg-Essen, Essen, Germany[6]

6 and German Cancer Consortium (DKTK)-University Hospital Essen, Essen, Germany

Word count abstract: 283; Word count manuscript: 5420

Corresponding author:
Dr. med. Christopher Darr
Resident urologist
Department of Urology
University hospital Essen
Hufelandstr. 55
45147 Essen, Germany
E-mail: christopher.darr@uk-essen.de
Phone.: 0049 201-723/85633
Fax.: 0049 201-723/3151

Abstract:

Objective: To assess the feasibility and accuracy of Cerenkov Luminescence Imaging (CLI) for assessment of surgical margins intraoperatively during radical prostatectomy (RPE).

Methods: A single centre feasibility study included 10 patients with high-risk primary prostate cancer (PC). ^{68}Ga-PSMA PET/CT scans were performed followed by RPE and intraoperative CLI of the excised prostate. In addition to imaging the intact prostate, in the first two patients the prostate gland was incised and imaged with CLI to visualise the primary tumour. We compared the tumour margin status on CLI to postoperative histopathology. Measured CLI intensities were determined as tumour to background ratio (TBR).

Results: Tumour cells were successfully detected on the incised prostate CLI images as confirmed by histopathology. 3 of 10 men had histopathological positive surgical margins (PSMs), and 2 of 3 PSMs were accurately detected on CLI. Overall, 25 (72%) out of 35 regions of interest (ROIs) proved to visualize a tumour signal according to standard histopathology. The median tumour radiance in these areas was 11301 photons/s/cm^2/sr (range 3328 - 25428 photons/s/cm^2/sr) and median TBR was 4.2 (range 2.1 – 11.6).

False positive signals were seen mainly at the prostate base with PC cells overlaid by benign tissue. PSMA-immunohistochemistry (PSMA-IHC) revealed strong PSMA staining of benign gland tissue, which impacts measured activities.

Conclusions: This feasibility showed that ^{68}Ga-PSMA CLI is a new intraoperative imaging technique capable of imaging the entire specimen's surface to detect PC tissue at the resection margin. Further optimisation of the CLI protocol, or the use of lower-energetic imaging tracers such as ^{18}F-PSMA, are required to reduce false positives. A larger study will be performed to assess diagnostic performance.

Key words: Cerenkov Luminescence Imaging, radio-guided surgery, prostate cancer, margin assessment, radical prostatectomy

Introduction:

Radical prostatectomy (RPE) is one of the primary treatment options for men with localized prostate cancer (PC) aiming for complete resection of the prostate without positive surgical margins (*1*). The *Pentafecta* outcome criteria for RPE include continence, potency, as well as lack of early complications, biochemical recurrence and positive surgical margins (PSMs), and should be fulfilled whenever oncologically possible (2).

Incomplete removal of the cancer tissue during RPE may be associated with poorer patient outcomes (3). A PSM increases the need for adjuvant radiotherapy, the likelihood of recurrence and the chances of PC-related mortality by a factor of three (3). PSMs of > 3 mm are known to increase the risk of biochemical recurrence (*4*). Similarly, men with persistently elevated PSA-levels ≥0.1 ng/mL more than six weeks after RPE show less favourable cancer control and survival rates over time (*5-7*).

Next to preoperative magnetic resonance imaging (MRI) for local staging of disease, and nomograms for the prediction of extracapsular extension, the use of intraoperative frozen-section analysis (IFS) can facilitate the surgeon's decision concerning preservation of functional structures like the neurovascular bundles (*1,8-10*).

Schlomm et al. described significantly less frequent PSM of 15% versus 22% for all stages and 21% versus 32% for extraprostatic disease, suggesting that systematic application of IFS has the potential to significantly increase nerve sparing and to reduce PSM in RPE. Other studies, however, demonstrated a high false-negative rate of IFS, potentially resulting in unjustified nerve-sparing surgery, and eminent time consumption (*8,11*). Consequently, there is a wish to be able to accurately detect malignant areas in real-time during RPE to ensure that the PC is completely removed. Molecular imaging with modern radiopharmaceuticals that target the prostate-specific membrane antigen (PSMA) can be used for highly specific and sensitive oncological diagnostic imaging, including initial staging of PC (*12-15*). PSMA positron emission tomography (PSMA-PET)

is an imaging technique that targets PSMA on PC cells, mostly with ^{68}Ga-labelled and ^{18}F-labelled PET-agents (*16*).

In recent trials, PSMA-PET demonstrated high detection rates of lymph nodes metastases and a positive predictive value for initial staging of PC (*17-20*). Maurer et al recently described the advantage of PSMA-radioguided surgery pelvic lymph node dissection, visualising even small lymph node metastasis (*21*).

PET imaging agents also emit optical photons via a phenomenon called Cerenkov luminescence, enabling optical molecular imaging in the form of Cerenkov Luminescence Imaging (CLI) (*22*). CLI and PET are directly correlated as both techniques measure photons: PET measures the gamma annihilation photons, and CLI measures the Cerenkov photons (*23*). Cerenkov photons are emitted by a charged particle (positron or electron) when travelling through a dielectric medium at a faster speed than the velocity of light in that medium. Although Cerenkov luminescence has a broadband wavelength spectrum, it predominantly comprises ultraviolet and blue light, and as these short wavelengths are highly attenuated in biological tissue, CLI is limited to detection of signals emitted in superficial tissue layers (approximately 3 mm). In contrast to PET, CLI is unable to detect photons emitted by deeper located tissues or tumours (*24,25*).

The clinical feasibility and safety of CLI have recently been demonstrated in a small number of breast cancer patients using ^{18}F-FDG (*24*). In this study, good agreement between CLI and histopathology was found for margin distance and invasive cancer tumour size.

To our knowledge there is no published data available regarding CLI in PC using a PSMA labelled tracer to date. Therefore, the aim of our prospective study was to analyse the feasibility and diagnostic accuracy of intraoperative CLI to detect PSM in a cohort of ten men undergoing RPE.

Patients and Methods

Patient Recruitment and Patient Preparation on Day of Surgery

Between February 2018 and June 2019, patients with histologically confirmed PC on systematic and/or MRI-targeted prostate biopsy were recruited at University Hospital Essen following discussion in the local multidisciplinary tumour board and written informed consent. This study received formal Ethical Committee approval (19-8749-BO). Exclusion criteria were previous prostate surgery or radiotherapy, known distant metastases, and contraindications to surgery.

On the day of surgery, ^{68}Ga-PSMA-11 (1.8-2.2 MBq per kg/body weight) was injected intravenously in patients scheduled to undergo RPE (*26*). After 45 to 60 minutes post-injection, the PET/CT scan was performed and assessed by experienced Nuclear Medicine physicians. In case of high-volume metastatic disease on PET/CT, same-day surgery would have been cancelled.

Radical Prostatectomy and Intraoperative CLI

Following PET/CT, RPE of these patients was performed by two surgeons ahead of extended pelvic lymph node dissection (ePLND) to minimize signal intensity reduction from radiotracer decay in the time between ^{68}Ga-PSMA injection and CLI. An indwelling catheter is immediately inserted in the operating theatre to drain the urine and minimize urinary contamination of the prostate. The excised prostate specimen was immediately retrieved from the abdomen, wiped to clear blood and fluids, positioned in a specimen tray and then imaged in the LightPath® CLI system (Lightpoint Medical Ltd., Chesham, UK). The LightPath® system captured both a Cerenkov image and a photographic image of the specimen in a light-tight imaging chamber and was positioned in the operating room to enable real-time image analysis by the surgeon. Images were acquired with a total acquisition time of 300 seconds and 8x8 pixel binning (*27*). The prostate gland was imaged in different positions, and a total of two or three images were necessary to capture all sides of the prostate. After the intact prostate was imaged, the prostate gland was incised in the first two

patients at the level of the main primary lesion on MRI, and subsequently imaged in CLI to visualise the primary tumour. Upon CLI completion, the prostatectomy specimen was sent for postoperative histopathological analysis. Due to the design of this feasibility study, the surgical course remained unaffected by the CLI results, and no further tissue was resected if positive margins were suspected on CLI.

Radiation safety

After completion of CLI, radiation safety monitoring was performed by accurately quantifying the activity in the excised prostate specimen using a high-purity Germanium detector (Canberra, Meridon, CT, USA). The activity was decay-corrected to the time of excision.

Image analysis

The Cerenkov luminescence images were analysed postoperatively in a controlled and standardized analysis environment using PMOD (PMOD Version 3.204, PMOD Technologies LLC). Measurements of the mean radiance (photons/s/cm^2/sr) were performed by drawing regions of interest (ROIs) on the Cerenkov luminescence images. ROIs were selected in areas showing increased signal intensity (tumour) and no increased signal (tissue background), and tumour to background ratios (TBRs) were calculated. Tumour margin assessment on CLI was performed by analysing elevated signals at the surface of the intact prostate images.

Histopathology and Immunhistochemistry

Histopathologic evaluation was performed adherent to the current German S3-guidelines for prostate cancer (*28*). RPEs were evaluated by expert uro-pathologists and typical prostate cancer metrics were reported including Gleason grading in its 2014 revision (*29*). PSMA-Immunohistochemistry (PSMA-IHC) was performed on an automated Ventana Benchmark Ultra device (Ventana Medical Systems) using PSMA antibody clone 3E6 (Agilent/DAKO, Santa Clara,

USA) with an 1:50 dilution. Membranous PSMA-expression in IHC-analyses was stratified according to its primary intensity of staining. Moderate and strong intensities were considered positive (*30*).

Results

In total 10 patients were included in the presented feasibility study. Patient characteristics are displayed in Table 1. Median age at surgery was 72 years, PSA 9.04 ng/ml and BMI 28.6. The median administered ^{68}Ga-PSMA activity was 119 MBq (range: 95 MBq to 202 MBq). The median time between intravenous injection and start of surgery was 223 minutes (range: 153 minutes to 328 minutes), and the median time between tracer injection and beginning of CLI acquisition was 333 minutes (range: 282 minutes to 429 minutes). The median decay-corrected tracer activity at CLI of the prostate was 0.34 kBq/mL (range: 0.13 and 3.1 kBq/mL; Table 2).

The incised prostate images acquired in the first two cases showed an elevated signal in the primary lesion as confirmed by histopathology (patient 1: TBR 2.95; patient 2: TBR lesion 1 4.89, TBR lesion 2 4.26) (Figure 1).

A total of 23 CLI images of the intact prostate were acquired and analysed in all 10 patients.

Patients 1, 5 and 6 had a PSM on histopathology (Table 1). In patient 1 and patient 5 the elevated signal levels enabled correct identification of these margins on CLI (Table 3, and Figure 2). International Society of Urological Pathology Gleason grade (ISUP-GG) at the resection margin were 5 (patient 1) with a diameter of 2 mm and 4 (patient 5) with a diameter of 8 mm. Tumour radiance and TBR were 19061 and 6.7 (patient 1), and 6131 and 1.9 (patient 5), respectively. In patient 6 no elevated signal could be identified on CLI, and this patient had an ISUP-GG 1 at the margin (right dorsal lobe) on histopathology with a diameter of 3 mm.

A total of thirty-five ROIs were drawn in areas displaying an elevated CLI signal; 24 in the base, 8 in the apex and 3 in the ventral side (Table 3). 25 out of the 35 ROIs (71.5%) were confirmed by pathology to contain tumour cells, however, some with margin distances of up to 3 mm. The median tumour radiance in these suspicious areas was 11301 photons/s/cm^2/sr (range 3328 - 25428 photons/s/cm^2/sr) and TBR 4.2 (range 2.1 – 11.6), respectively.

PSMA-IHC was performed in the last slices of the prostate base in the first 8 patients where standard histopathology suggested false positive results to assess PSMA expression in these

areas (Figure 3, Table 4). PSMA-IHC demonstrated a moderate to strong PSMA-IHC signal that corresponded to CLI in benign tissue in 7 out of 8 patients. In 5 (62.5%) patients underlying PC tissue with PSMA-IHC expression was also observed. All cancer areas showed an elevated CLI-intensity.

In 4 patients radiation safety measurements were performed which demonstrated that the intensity level in the excised specimen are below the permitted exemption levels stipulated by the German radiation protection ordinance (^{68}Ga < 100 kBq).

Discussion

This first-in-man study evaluated the feasibility of intraoperative ^{68}Ga-PSMA CLI for assessing tumour margin status in patients with high-risk primary PC undergoing RPE and ePLND. CLI seems to be able to successfully detect positive histopathological resection margins with high ISUP-GG, and all ROIs containing PSMA-IHC positive cancer tissue showed elevated Cerenkov intensity. The low ^{68}Ga-PSMA activity at the time of surgery implies that the prostate specimen presents no considerable radiation burden for the CLI operator and pathologist and can be treated as non-radioactive material.

One patient had a PSM containing ISUP-GG 1, but this margin did not display an increased signal on CLI. As these low-grade cancers are known to have a lower PSMA expression, this may be an explanation for a false-negative CLI result (*30*).

To further examine Cerenkov signals the prostate gland was incised at the main tumour lesion in two patients. In both patients two suspicious areas were detected. Correlation of histopathology and CLI proved a detection rate of 100% in patient 2 and 50% in patient 1, respectively. Here superficial cancer cells are described on the left side. Due to the main cancer nidus at the right dorsal prostate base, we assume that the cancer tissue was overlaid through a thin layer of normal tissue and could therefore be not visualized in CLI. This assumption is supported through a higher TBR of the left ROI (2.95 vs. 2.46).

Although ^{68}Ga-PSMA CLI of prostatectomy specimens seems feasible for assessing tumour resection margin status, 10 of the 35 ROIs showed elevated signal levels without histopathological evidence of PC tissue at the resection margin. There are several reasons that could explain these false-positive findings. Firstly, CLI intensity can emerge from PSMA-expression and tracer uptake in non-cancerous tissues. To analyse the prostate base where CLI was positive despite negative histopathology, PSMA-IHC of the last slice of the prostate base was performed in 8 patients. Here, in 14/16 (87%) areas a PSMA staining of benign tissue was observed. Eight of these may have caused a false-positive signal on CLI as they were close to the tissue's surface. Secondly, the

mean positron range of ^{68}Ga is ±2.8mm (*31*), and thus Cerenkov luminescence can be produced from a few millimetres underneath the tissue's surface. To enable more superficial imaging a shortpass optical filter might be used in the future to exclude the longer-wavelength Cerenkov photons that have a deeper tissue penetration (i.e. the red and near-infrared Cerenkov photons). Another option would be to use a ^{18}F-labelled PSMA tracer such as ^{18}F-PSMA-1007 (*17*). As ^{18}F positrons have a lower energy compared to ^{68}Ga (0.64 MeV vs 1.9 Mev), the mean positron range in tissue is significantly shorter (0.54 vs 2.83 mm), thus facilitating submillimetre margin assessment (*31*). Lastly, ^{68}Ga-PSMA-11 is known to be excreted via the urinary tract, and thus could cause elevated signals at the bladder neck or prostate base through urinary contamination (*32*). One method for minimising the risk of prostate surface contamination from urine is to rinse the prostate with sodium chloride prior to CLI image acquisition. However, this was not performed in this study. Another solution would be to use a tracer that has nonrenal clearance such as ^{18}F-PSMA-1007 (*17,33*).

The pre-clinical study by Olde Heuvel et al. found 0.14 kBq/mL as the minimum detectable intensity for a 300s 8x8 binning acquisition (*34*). Due to the long interval between tracer injection and CLI in our study (~6 hours), the activity levels in the prostate at the time of CLI were low (median ^{68}Ga-PSMA activity of 0.34 kBq/mL) and close to the limit of detection. To avoid a loss of imaging quality a long acquisition time is essential. Despite this, tumour margin assessment on CLI could be performed in all 10 patients. To increase the difference in CLI signal intensity between benign and PC tissue, the time from injection to CLI can be reduced, which may improve the detectability of low-avid PSMA cancers including low ISUP-GG. Alternatively, the workflow could be changed so that at the day of surgery no PET imaging is performed, but only a reduced amount of tracer injected.

Long-term prediction of prostate cancer-specific mortality is mainly based on histopathology features as described by Eggener et al. Poorly differentiated cancer, with a Gleason-Score of 8-10, and seminal vesicle invasion are prime determinants of prostate cancer specific mortality after

radical prostatectomy (*35*). Findings of Martini et al. demonstrate that only unfavorable positive surgical margins (≥3 mm and/or multifocal positive margins) have a significant influence on risk of metastasis in prostate cancer (*36*). Up to date intraoperative frozen section analysis is the gold standard to assess removal of all prostate cancer tissue. If addition of shortpass optical filters reduces the penetration depth of CLI, frozen section analysis might be reduced to conspicuous areas only in the future.

To assess sensitivity and specificity a single centre clinical study is scheduled to commence in early 2020. The recruitment target is 40 patients with the first patient expected to be recruited in Q1 2020. In these patients the CLI protocol will be improved by implementing a shortpass optical filter. In parallel to the planned clinical study we are performing preclinical experiments using 3D printed prostate models to evaluate penetration depth and resolution of CLI in correlation with tracer activity levels.

CLI employs nuclear medicine methods to inform urologic surgery for improved local treatment of prostate cancer. This new imaging modality brings the urology and nuclear medicine communities more closely together to make progress in prostate cancer (*37*).

Conclusions

Intraoperative ^{68}Ga-PSMA CLI in PC is a promising tool to improve surgery. CLI provides high-resolution information of the whole prostate gland that may allow surgeons to assess margin status with a good correlation to histopathologic examination.

M Grootendorst in an employee of Lightpoint Medical Ltd. Wolfgang P. Fendler is a consultant for Ipsen, Endocyte, and BTG, and he received personal fees from RadioMedix outside of the submitted work. The other authors declare that no relevant conflict of interest relevant to this article exists.

Key-Points

Question: Is Cerenkov Luminescence Imaging (CLI) useful for displaying prostate cancer cells close to or at the surface of prostatectomy specimen?

Pertinent findings: In this feasibility study 10 patients undergoing radical prostatectomy with a ^{68}Ga-PET/CT scan on the same day were analysed for suspicious intensity levels. CLI was able to detect cancer cells close to and at the surface of the prostate. These results are the basis to initiate further prospective studies.

Implications for patient care: CLI is a promising technique for intraoperative evaluation of the whole prostate surface regarding positive surgical margins.

References

1. EAU Guidelines. Edn. presented at the EAU Annual Congress Barcelona 2019.

2. Patel VR, Sivaraman A, Coelho RF, et al. Pentafecta: a new concept for reporting outcomes of robot-assisted laparoscopic radical prostatectomy. *Eur Urol.* 2011;59:702-707.

3. Wright JL, Dalkin BL, True LD, et al. Positive surgical margins at radical prostatectomy predict prostate cancer specific mortality. *J Urol.* 2010;183:2213-2218.

4. Kozal S, Peyronnet B, Cattarino S, et al. Influence of pathological factors on oncological outcomes after robot-assisted radical prostatectomy for localized prostate cancer: Results of a prospective study. *Urol Oncol.* 2015;33:330.e331-337.

5. Rogers CG, Khan MA, Craig Miller M, Veltri RW, Partin AW. Natural history of disease progression in patients who fail to achieve an undetectable prostate-specific antigen level after undergoing radical prostatectomy. *Cancer.* 2004;101:2549-2556.

6. Bianchi L, Nini A, Bianchi M, et al. The Role of Prostate-specific Antigen Persistence After Radical Prostatectomy for the Prediction of Clinical Progression and Cancer-specific Mortality in Node-positive Prostate Cancer Patients. *Eur Urol.* 2016;69:1142-1148.

7. Preisser F, Chun FKH, Pompe RS, et al. Persistent Prostate-Specific Antigen After Radical Prostatectomy and Its Impact on Oncologic Outcomes. *Eur Urol.* 2019.

8. Schlomm T, Tennstedt P, Huxhold C, et al. Neurovascular structure-adjacent frozen-section examination (NeuroSAFE) increases nerve-sparing frequency and reduces positive surgical margins in open and robot-assisted laparoscopic radical prostatectomy: experience after 11,069 consecutive patients. *Eur Urol.* 2012;62:333-340.

9. Nyarangi-Dix J, Wiesenfarth M, Bonekamp D, et al. Combined Clinical Parameters and Multiparametric Magnetic Resonance Imaging for the Prediction of Extraprostatic Disease-A Risk Model for Patient-tailored Risk Stratification When Planning Radical Prostatectomy. *Eur Urol Focus.* 2018.

10. Petralia G, Musi G, Padhani AR, et al. Robot-assisted radical prostatectomy: Multiparametric MR imaging-directed intraoperative frozen-section analysis to reduce the rate of positive surgical margins. *Radiology.* 2015;274:434-444.

11. Gillitzer R, Thuroff C, Fandel T, et al. Intraoperative peripheral frozen sections do not significantly affect prognosis after nerve-sparing radical prostatectomy for prostate cancer. *BJU Int.* 2011;107:755-759.

12. Perera M, Papa N, Roberts M, et al. Gallium-68 Prostate-specific Membrane Antigen Positron Emission Tomography in Advanced Prostate Cancer-Updated Diagnostic Utility,

Sensitivity, Specificity, and Distribution of Prostate-specific Membrane Antigen-avid Lesions: A Systematic Review and Meta-analysis. *Eur Urol.* 2019.

13. Yaxley JW, Raveenthiran S, Nouhaud FX, et al. Risk of metastatic disease on (68) gallium-prostate-specific membrane antigen positron emission tomography/computed tomography scan for primary staging of 1253 men at the diagnosis of prostate cancer. *BJU Int.* 2019;124:401-407.

14. Koschel S, Murphy DG, Hofman MS, Wong LM. The role of prostate-specific membrane antigen PET/computed tomography in primary staging of prostate cancer. *Curr Opin Urol.* 2019;29:569-577.

15. Kalapara AA, Nzenza T, Pan HY, et al. Detection and localisation of primary prostate cancer using (68) Ga-PSMA PET/CT compared with mpMRI and radical prostatectomy specimens. *BJU Int.* 2019.

16. Schwarzenboeck SM, Rauscher I, Bluemel C, et al. PSMA ligands for PET imaging of prostate cancer. *J Nucl Med.* 2017;58:1545-1552.

17. Kesch C, Vinsensia M, Radtke JP, et al. Intraindividual Comparison of (18)F-PSMA-1007 PET/CT, Multiparametric MRI, and Radical Prostatectomy Specimens in Patients with Primary Prostate Cancer: A Retrospective, Proof-of-Concept Study. *J Nucl Med.* 2017;58:1805-1810.

18. Giesel FL, Hadaschik B, Cardinale J, et al. F-18 labelled PSMA-1007: biodistribution, radiation dosimetry and histopathological validation of tumor lesions in prostate cancer patients. *Eur J Nucl Med Mol Imaging.* 2017;44:678-688.

19. Herlemann A, Wenter V, Kretschmer A, et al. (68)Ga-PSMA Positron Emission Tomography/Computed Tomography Provides Accurate Staging of Lymph Node Regions Prior to Lymph Node Dissection in Patients with Prostate Cancer. *Eur Urol.* 2016;70:553-557.

20. van Kalmthout LWM, van Melick HHE, Lavalaye J, et al. Prospective Validation of Gallium-68 PSMA-PET/CT in Primary Staging of Prostate Cancer Patients. *J Urol.* 2019:101097ju0000000000000531.

21. Maurer T, Weirich G, Schottelius M, et al. Prostate-specific membrane antigen-radioguided surgery for metastatic lymph nodes in prostate cancer. *Eur Urol.* 2015;68:530-534.

22. Das S, Thorek DL, Grimm J. Cerenkov imaging. *Adv Cancer Res.* 2014;124:213-234.

23. Grootendorst MR, Cariati M, Kothari A, Tuch DS, Purushotham A. Cerenkov luminescence imaging (CLI) for image-guided cancer surgery. *Clin Transl Imaging.* 2016;4:353-366.

24. Grootendorst MR, Cariati M, Pinder SE, et al. Intraoperative Assessment of Tumor Resection Margins in Breast-Conserving Surgery Using (18)F-FDG Cerenkov Luminescence Imaging: A First-in-Human Feasibility Study. *J Nucl Med.* 2017;58:891-898.

25. Chin PT, Welling MM, Meskers SC, Valdes Olmos RA, Tanke H, van Leeuwen FW. Optical imaging as an expansion of nuclear medicine: Cerenkov-based luminescence vs fluorescence-based luminescence. *Eur J Nucl Med Mol Imaging.* 2013;40:1283-1291.

26. Fendler WP, Eiber M, Beheshti M, et al. (68)Ga-PSMA PET/CT: Joint EANM and SNMMI procedure guideline for prostate cancer imaging: version 1.0. *Eur J Nucl Med Mol Imaging.* 2017;44:1014-1024.

27. Ciarrocchi E, Vanhove C, Descamps B, De Lombaerde S, Vandenberghe S, Belcari N. Performance evaluation of the LightPath imaging system for intra-operative Cerenkov luminescence imaging. *Phys Med.* 2018;52:122-128.

28. Leitlinienprogramm Onkologie (Deutsche Krebsgesellschaft, Deutsche Krebshilfe, AWMF): Interdisziplinäre Leitlinie der Qualität S3 zur Früherkennung, Diagnose und Therapie der verschiedenen Stadien des Prostatakarzinoms, Langversion 5.1, 2019, AWMF Registernummer: 043/022OL, http://www.leitlinienprogramm-onkologie.de/leitlinien/prostatakarzinom/. Accessed 24.06.2019.

29. Epstein JI, Egevad L, Amin MB, Delahunt B, Srigley JR, Humphrey PA. The 2014 International Society of Urological Pathology (ISUP) Consensus Conference on Gleason Grading of Prostatic Carcinoma: Definition of Grading Patterns and Proposal for a New Grading System. *Am J Surg Pathol.* 2016;40:244-252.

30. Hupe MC, Philippi C, Roth D, et al. Expression of Prostate-Specific Membrane Antigen (PSMA) on Biopsies Is an Independent Risk Stratifier of Prostate Cancer Patients at Time of Initial Diagnosis. *Front Oncol.* 2018;8:623.

31. Moses WW. Fundamental Limits of Spatial Resolution in PET. *Nucl Instrum Methods Phys Res A.* 2011;648 Supplement 1:S236-s240.

32. Budaus L, Leyh-Bannurah SR, Salomon G, et al. Initial Experience of (68)Ga-PSMA PET/CT Imaging in High-risk Prostate Cancer Patients Prior to Radical Prostatectomy. *Eur Urol.* 2016;69:393-396.

33. Giesel FL, Will L, Kesch C, et al. Biochemical Recurrence of Prostate Cancer: Initial Results with [(18)F]PSMA-1007 PET/CT. *J Nucl Med.* 2018;59:632-635.

34. Olde Heuvel J, de Wit-van der Veen BJ, Vyas KN, et al. Performance evaluation of Cerenkov luminescence imaging: a comparison of (68)Ga with (18)F. *EJNMMI Phys.* 2019;6:17.

35. Eggener SE, Scardino PT, Walsh PC, et al. Predicting 15-year prostate cancer specific mortality after radical prostatectomy. *J Urol.* 2011;185:869-875.

36. Martini A, Gandaglia G, Fossati N, et al. Defining Clinically Meaningful Positive Surgical Margins in Patients Undergoing Radical Prostatectomy for Localised Prostate Cancer. *Eur Urol Oncol.* 2019.

37. Murphy DG, Hofman MS, Azad A, Violet J, Hicks RJ, Lawrentschuk N. Going nuclear: it is time to embed the nuclear medicine physician in the prostate cancer multidisciplinary team. *BJU Int.* 2019.

#	Age at surgery (years)	ISUP-GG at PBx	PSA (ng/ml)	BMI (kg/m^2)	T-category	N-category	R-Status	Location of PSM/ Comment on histopathology	ISUP-GG	ISUP-GG at R1
1	76	5	10.6	24.2	pT3b	pN1	R1	Dorsal, right base (2 mm)	4	5
2	71	4	3.3	25.9	pT3a	pN0	R0		5	
3	75	5	14.1	30.1	pT3b	pN1	R0		5	
4	76	3	6.9	23.4	pT2a	pN0	R0		3	
5	66	4	77.7	30.6	pT3a	pN1	R1	Left apical lobe (8 mm)	5	4
6	63	4	5.3	35.9	pT2c	pN0	R1	Dorsal, right lobe (3 mm)	3	1
7	81	4	11.4	27.1	pT3a	pN0	R0		3	
8	72	3	7.1	31.6	pT3a	pN0	R0		2	
9	63	5	20	32.1	pT3b	pN1	R0		5	
10	68	5	7.48	26.9	pT3a	pN0	R0		2	

Table 1. Patient and oncological characteristics. BMI: body-mass-index, ISUP-GG: International Society of Urological Pathology Gleason grade, PBx: prostate biopsy, PSA: prostate specific antigen, PSM: positive surgical margin, Grey filled fields: Not applicable.

#	Tracer activity at injection (MBq)	Duration until surgery (minutes)	Duration until CLI (minutes)	Maximum tracer activity concentration at CLI (kBq/mL)*
1	202	193	313	2.37
2	95	229	340	0.42
3	108	285	429	0.14
4	150	153	285	3.07
5	163	217	282	2.80
6	118	192	304	0.40
7	103	199	326	0.81
8	97	292	391	0.13
9	121	325	420	0.18
10	157	328	409	0.16

Table 2. Overview of injected activity and the duration between injection, surgery and CLI per patient. CLI: Cerenkov Luminescence Imaging, kBq: Kilo Becquerel, MBq: Mega Becquerel.
* Based on the preoperative ^{68}Ga-PSMA PET/CT decay-corrected to the time of CLI

#	Placement	Prostate tissue background	ROI 1	ROI location 1	ROI 2	ROI location 2	ROI 3	ROI Location 3	ROI 4	ROI location 4
1	Base down	1895 (±343)	**6101 (±743) TBR: 3.22**	**Dorsal, left base**	7376 (±1628) TBR: 3.89	Right ventral apex				
	Posterior down	2845 (±357)	**12409 (±4040) TBR: 4.36**	**Whole base**	7900 (±1461) TBR: 2.78	Ventral central	**19061 (±3689) TBR: 6.7**	**Right base**		
	Posterior down *(Incised base)*	2192 (±319)	**6468 (±1207) TBR: 2.95**	**Left base incised**	5400 (±745) TBR: 2.46	Right base incised				
2	Ventral down	1507 (±209)	**5106 (±1482) TBR: 3.39**	**Right base**						
	Posterior down	2426 (±285)	**11383 (±5591) TBR: 4.69**	**Whole base**	9802 (±1922) TBR: 4.04	Ventral central	**19399 (±3079) TBR: 8.0**	**Right base**	**22350 (±4464) TBR: 9.21**	**Left base**
	Posterior down *(Incised base)*	2155 (±353)	**10538 (±2567) TBR: 4.89**	**Left base incised**	**9188 (±1752) TBR: 4.26**	**Right base incised**	10239 (±2378) TBR: 4.75	Ventral central		
3	Posterior down	1695 (±333)	5035 (±1008) TBR: 2.97	Left base						
	Base down	1949 (±345)								
4	Posterior down	2001 (±275)	**8069 (±2676) TBR: 4.03**	**Central base**	6031 (±1285) TBR: 3.01	Ventral apex				
	Base down	1651 (±287)	**3526 (±877) TBR: 2.14**	**Dorsal, left base**	5376 (±1265) TBR: 3.26	Ventral apex				
5	Apex down	5310 (±1447)	**18664 (±5258) TBR: 3.51**	**Central base**	**25428 (±4351) TBR: 4.79**	**Left base**				
	Posterior down	3219 (±504)	**6131 (±1686) TBR: 1.9**	**Left ventral apex**	**6242 (±1984) TBR: 1.94**	**Right and left base**				
	Ventral down	1663(±231)	**3328 (±535) TBR: 2.0**	**Dorsal base left>right**						
6	Apex down	1967 (±293)	9964 (±2718) TBR: 5.07	Right base	5146 (±2378) TBR: 2.62	Central base				
	Posterior down	1650 (±256)	**3436 (±793) TBR: 2.08**	**Apex ventral**						
7	Base down	2559 (±520)	**8888 (±1867) TBR: 3.47**	**Apex ventral**						
	Posterior down	2390 (±533)	**28048 (±5403) TBR: 11.59**	**Right base**	6846 (±2178) TBR: 5.86	Left base				
8	Posterior down	2847 (±514)	**18565 (±4056) TBR: 6.52**	**Right base**	**20282 (±2979) TBR: 7.12**	**Left base**				
	Base down	1739 (±260)								
	Ventral down	1715 (±288)								
9	Posterior down	3105 (±444)	**13039 (±3850) TBR: 4.20**	**Left base**	**11716 (±2991) TBR: 3.77**	**Central base**				
	Base down	2528 (±364)								
10	Ventral down	1742 (±295)								
	Base down	1832 (±278)	**4205 (±1023) TBR: 2.3**	**Apex ventral**						
	Posterior Down	2662 (±407)	**24520 (±6428)**	**Right base**	**23969 (±5235)**	**Left base**	**11218 (±4251)**	**Ventral apex**		

			TBR: 9.21		**TBR: 9.0**		**TBR: 4.21**			

Table 3. Cerenkov Luminescence Imaging measurements. Elevated Cerenkov-Luminescence activities with histopathological proof of prostate cancer tissue in the respective regions are marked bold (< 3mm). Regions in which histopathological positive resection margins were detected are underlined. Activity levels are stated in photons/s/cm^2/sr and as mean (± standard deviation). ROI: region of interest, TBR: Tumour to background ratio. Grey filled fields: Not applicable.

#	Anatomical region	PSMA-IHC expression carcinoma	PSMA-IHC expression benign
1	Right lobe, prostate base	negative	positive
	Left lobe, prostate base	positive	positive
	Transition to left seminal vesicle	positive	positive
	Transition to right seminal vesicle	negative	positive
2	Right lobe, prostate base	positive	positive
	Transition to right seminal vesicle	negative	positive
	Transition to left seminal vesicle	negative	positive
3	Right bladder neck	negative	positive
	Left bladder neck	negative	positive
4	Right lobe, prostate base	negative	positive
	Left lobe, prostate base	negative	positive
	Right bladder neck	negative	positive
	Left bladder neck	negative	positive
5	Transition to right seminal vesicle	positive	negative
	Transition to left seminal vesicle	positive	negative
6	Right lobe, prostate base	negative	positive
	Left lobe, prostate base	negative	positive
7	Transition to right seminal vesicle	positive	positive
	Transition to left seminal vesicle	negative	positive
	Right bladder neck	negative	positive
	Left bladder neck	negative	positive
8	Right lobe, prostate base	negative	positive
	Left lobe, prostate base	positive	positive
	Transition to left seminal vesicle	positive	positive
	Transition to right seminal vesicle	negative	positive

Table 4. PSMA-Immunohistochemistry (PSMA-IHC). For further analysis of the prostate base, selectively staining of the last slices of the prostate base was performed. A positive result indicated a moderate to strong PSMA-expression. PSMA-IHC: prostate-specific membrane antigen immunohistochemistry.

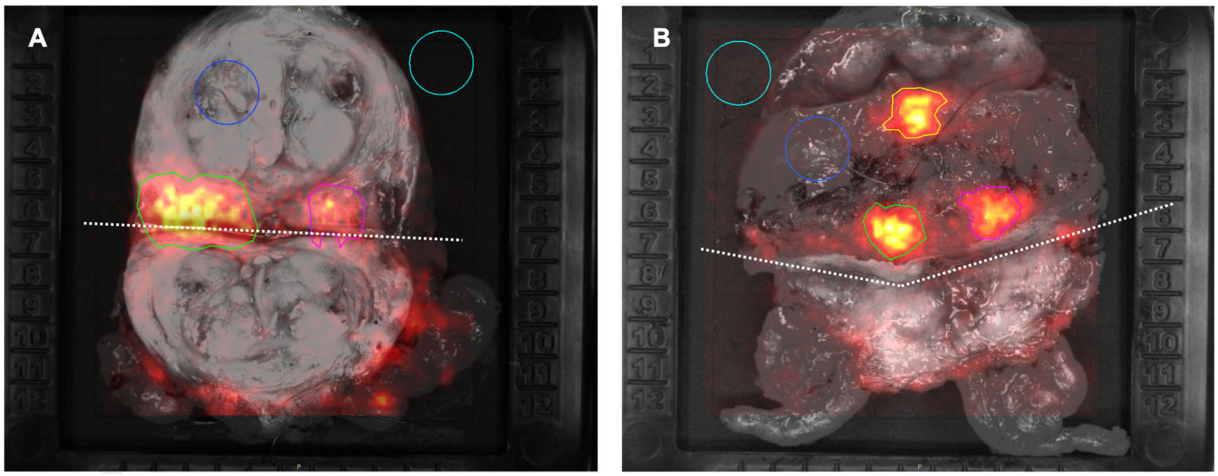

Figure 1. Grey-scale photographic images overlaid with Cerenkov signals. Incised prostate gland specimen of patient number 1 (A) and 2 (B). In each image the ROIs are encircled. The incision is marked with a dotted line. The light blue ROI (area of empty specimen tray) and dark blue ROI (area of normal prostate tissue) were used as empty background and tissue background, respectively. The green ROI (lesion 1) and pink ROI (lesion 2) show an increased signal; histopathological analysis confirmed cancer tissue in these areas. The orange ROI in image B shows an increased signal from an area without cancer cells.

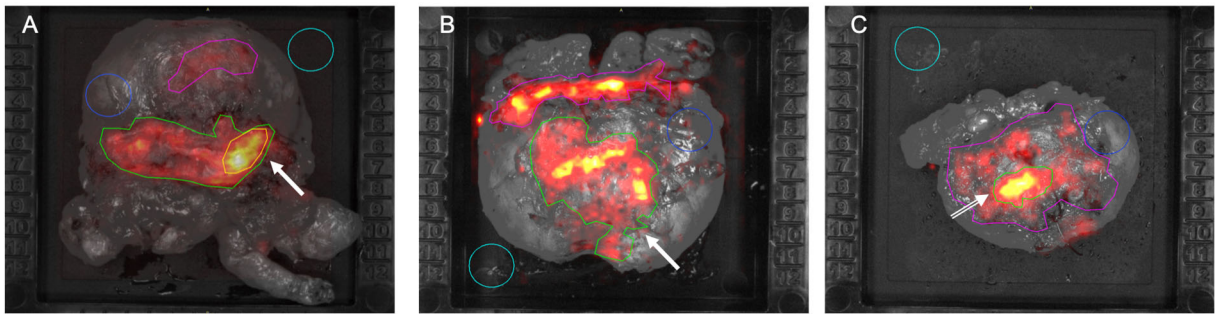

Figure 2. Grey-scale photographic images overlaid with Cerenkov signal for patients with positive surgical margins (A: patient 1, B: patient 5, C: patient 6). Elevated signal (white arrow) from tumour can be seen in A and B. Elevated signal without histopathological tumour cell correlation displayed in C (white dashed arrow). Immunohistochemistry showed PSMA expression of benign tissue in this region.

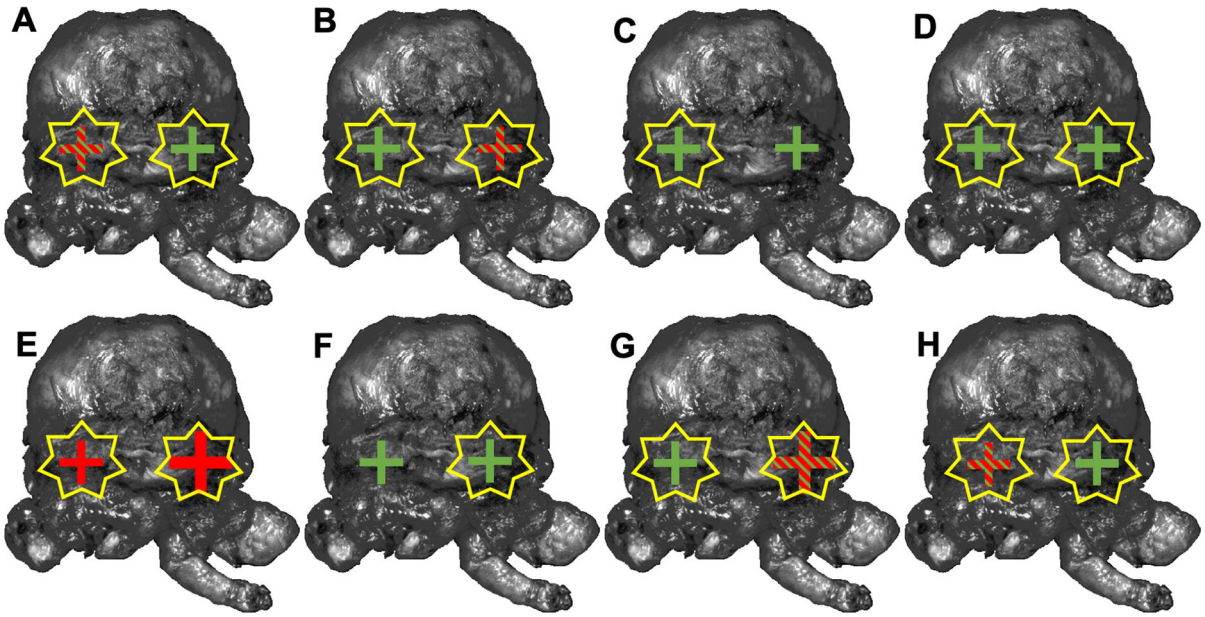

Figure 3. PSMA-Immunohistochemistry (PSMA-IHC) correlation of the prostate base. Running from A: patient 1 to H: patient 8. Green Cross = PSMA-IHC expression benign gland tissue, Red Cross = PSMA-IHC expression carcinoma, Green and red striped Cross = PSMA-IHC expression benign gland tissue and carcinoma. The crosses display the analysed side (left or right prostate base). Additionally, bigger crosses symbolize a high amount of tumour cells. The yellow star displays increased Cerenkov intensity in this area. PSMA-IHC: prostate-specific membrane antigen immunohistochemistry.